A Tetraphenylethylene Core-Based 3D Structure Small Molecular Acceptor Enabling Efficient Non-Fullerene Organic Solar Cells

*Yuhang Liu, Cheng Mu, Kui Jiang, Jingbo Zhao, Yunke Li, Lu Zhang, Zhengke Li, Joshua Yuk Lin Lai, Huawei Hu, Tingxuan Ma, Rongrong Hu, Demei Yu, Xuhui Huang, Ben Zhong Tang, and He Yan**

Bulk heterojunction (BHJ) organic solar cells (OSCs) have attracted much research attention due to their promise in low-cost conversion of solar energy.[1–5] A common BHJ OSC consists of an electron donor and an electron acceptor that work together to convert light to electricity.[2,3] To date, best-performance OSCs can only be achieved using a specific type of acceptor materials, fullerenes (e.g., [6,6]-phenyl-C61-butyric acid methyl ester [PCBM]).[4,5] Fullerenes work particularly well for BHJ OSCs, because they have ball or near-ball-shape structures and can thus readily form a 3D charge-transporting network.[6,7] In addition, commonly used fullerene derivatives ($PC_{61}BM$ or $PC_{71}BM$) can form reasonably small fullerene domains (20 nm) in BHJ films, yet still provide a sufficient electron-transport mobility (space-charge-limited-current [SCLC] and field-effect transistor [FET] electron mobilities of $PC_{61}BM$ are $\approx 2 \times 10^{-3}$ and 2.8×10^{-2} cm^2 V^{-1} s^{-1}, respectively)[8,9] for OSCs. Small domain size and sufficient electron mobility are two important requirements to achieve high-performance OSCs.[10] Despite their high performance, fullerenes have several drawbacks such as poor absorption properties and high costs of purification and production.[11] For this reason, non-fullerene acceptor materials including small molecules (SMs)[6,7,12–25] and conjugated polymers[26–30] have been actively explored as potential alternatives to replace fullerenes in OSCs.

In contrast to PCBM, it is much more challenging for SM acceptors to achieve small domain sizes and sufficient electron mobilities at the same time. A common problem for SM acceptor materials is that many crystalline SM materials with large planar structures tend to form excessively large crystalline domains (as large as 1 μm) in BHJ films.[15,19] To prevent the aggregation of SM acceptors, SMs with twisted structures or with bulky bridging units have been developed.[15,19,21,22] The twisted or bulky groups reduce intermolecular interactions and thus molecular aggregations. These SMs can form smooth amorphous BHJ films with reasonably small domain sizes. However, commonly used amorphous SM acceptor materials exhibit relatively low electron mobilities mostly on the order of 10^{-5} or 10^{-4} cm^2 V^{-1} s^{-1}[14,18,19,21,24] (determined by the SCLC method). Furthermore, most SM acceptors do not have the 3D ball-shape molecular structure of fullerenes and thus may not form a 3D charge-transporting network as readily as fullerenes do. For this reason, a potentially promising approach is to develop SM materials with quasi-3D or 3D molecular structures. Zhan and co-workers[21] have demonstrated a star-shape trimer that has a quasi-3D molecular structure, which has enabled interesting material properties and reasonably high-performing SM acceptor-based OSCs.

This paper reports a tetraphenylethylene (TPE) core-based SM acceptor, TPE-PDI_4, with a unique 3D molecular structure that enables the construction of non-fullerene OSCs with a high power-conversion efficiency (PCE) of 5.53%. TPE is a building block widely used in the field of aggregation-induced emission (AIE).[31,32] While the light-emitting properties of TPE-based molecules are not relevant to this paper, TPE does exhibit some special properties suitable for the OSC application. Its four phenyl rings are highly twisted due to strong steric hindrance: they all tilt by about 50° relative to the plane of the center double bond and form a "four-wing propeller-shape" molecular structure (**Figure 1**a) in the solid state.[33] Due to their highly twisted molecular structure, TPE-based molecules exhibit weak intermolecular interactions and thus excellent solubility in organic solvents even when they have no or very minimal alkyl-solubilizing groups. Given these properties, in this study, the TPE core structure is connected to four perylenediimide (PDI) units, which have a very large near-planar structure and are commonly used as the acceptor for non-fullerene OSCs.[34,35] The 2D chemical structure of TPE-PDI_4 is shown in Figure 1b. To obtain the 3D molecular conformations of TPE-PDI_4, density functional theory (DFT) calculations have performed. Figure 1c–e illustrates three possible locally optimal structural conformations of TPE-PDI_4, which all exhibit 3D molecular structures. In Figure 1c, the two PDIs on the same side (left or right) of the TPE double bond exhibit an "edge-to-face" geometry. In Figure 1d, the two PDIs on the same side are

Y. Liu, Dr. C. Mu, K. Jiang, J. Zhao, Y. Li, Dr. L. Zhang, Z. Li, J. Y. L. Lai, H. Hu, T. Ma, Dr. R. Hu, Prof. X. Huang, Prof. B. Z. Tang, Prof. H. Yan
Department of Chemistry
The Hong Kong University of Science and Technology
Clear Water Bay, Hong Kong
E-mail: hyan@ust.hk

Dr. R. Hu, Prof. X. Huang, Prof. B. Z. Tang, Prof. H. Yan
HKUST Shenzhen Research Institute
No. 9 Yuexing 1st RD, Hi-tech Park, Nanshan, Shenzhen 518057, China

Y. Liu, T. Ma, Prof. D. Yu
Joint School of Sustainable Development and MOE Key Lab for Non-Equilibrium Synthesis and Modulation of Condensed Matter.
Xi'an Jiaotong University
Xi'an 710049, P R China

DOI: 10.1002/adma.201404152

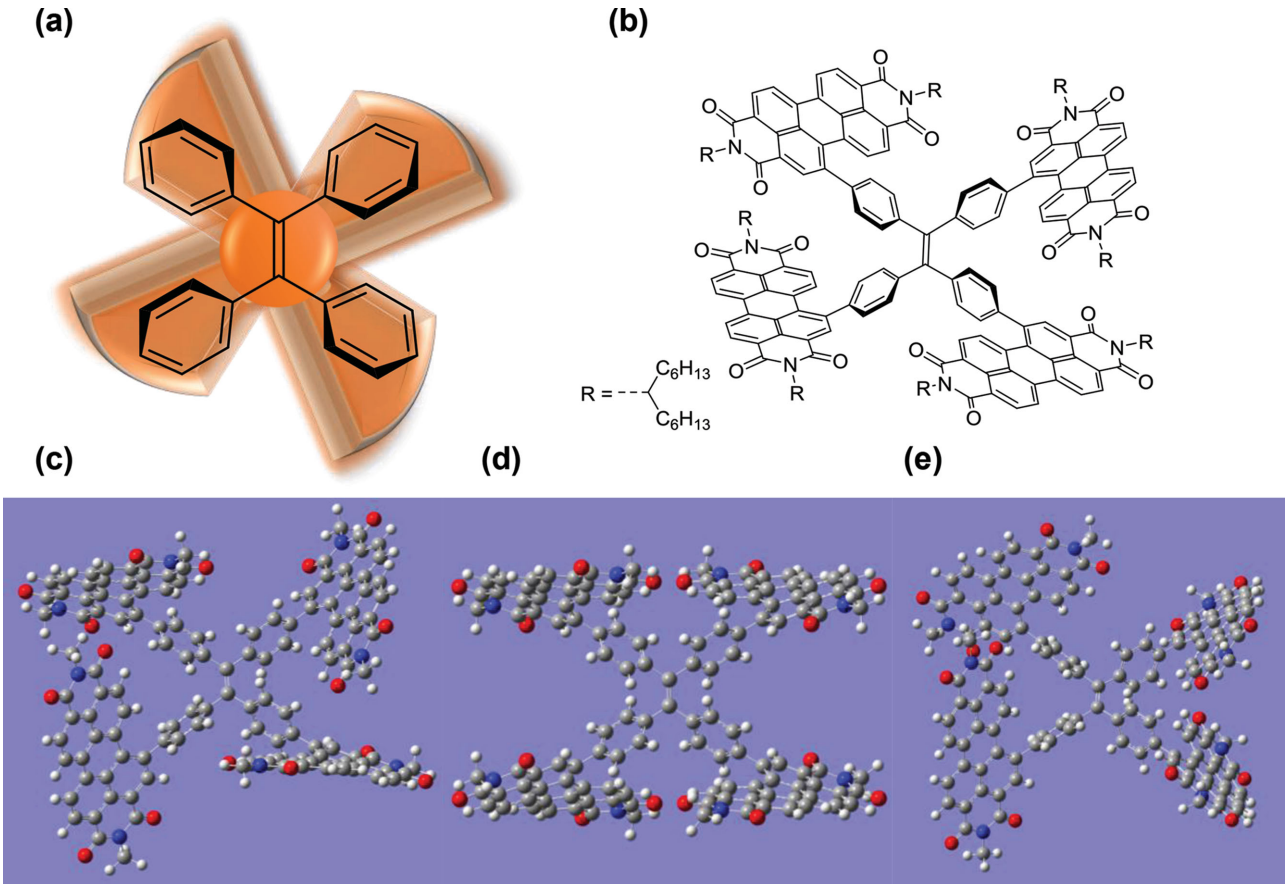

Figure 1. a) The "four-wing propeller-shape" molecular structure of TPE; b) Chemical structure of TPE-PDI_4; and c–e) Three possible structural conformations of TPE-PDI_4.

mostly parallel. In the conformation shown in Figure 1e, the two PDIs on the left side exhibit the "edge-to-face" geometry, and those on the right side form a 90° "L-shape" geometry.

Despite its very large molecular weight, TPE-PDI_4 exhibits excellent solubility in common organic solvents (e.g., THF, CH_2Cl_2, etc.) and is even soluble in hexane, which results from its highly twisted nonplanar 3D molecular structure and a proper choice of alkyl chains. With great solubility, TPE-PDI_4 can be solution processed (e.g., spincast) into very smooth thin films. The atomic force microscopy (AFM) image of a spin-casted TPE-PDI_4 film in **Figure 2**b shows a smooth surface with a root-mean-square roughness of 0.207 nm. Characterized by XRD, the TPE-PDI_4 film is shown to be amorphous in Figure 2a. It is well known that PDI has a large near-planar structure and strong tendency to aggregate and thus forms crystalline films with large-size surface features. PDI-based molecules used as acceptors in OSCs must include structural features that prevent the strong crystallization of PDIs, such as bulky and twisted bridging groups. The fact that TPE-PDI_4 forms ultra-smooth and amorphous films with featureless surfaces indicates that the TPE core structure is highly effective in reducing the aggregation tendency of the PDI units, which makes TPE-PDI_4 a suitable candidate acceptor for BHJ OSCs.

BHJ OSC devices have been fabricated using PBDTT-F-TT (**Figure 3**a) as the donor[24,36] and TPE-PDI_4 as the acceptor. The AFM images of the PBDTT-F-TT:TPE-PDI_4 blend film in Figure 2c show surface features with sizes of ≈20–30 nm, confirming that TPE-PDI_4 does not form large acceptor domains in the BHJ film. While many of the device parameters are not optimized, initial device-fabrication attempts have yielded an impressive power-conversion efficiency of 5.53% (Figure 3c, **Table 1**), placing them among the best-performing SM acceptor-based OSCs reported to date.[6,20,21,23–25] The V_{oc} of the PBDTT-F-TT:TPE-PDI_4-based cells is ≈0.91 V, which is significantly higher than that of PBDTT-F-TT:PCBM-based cells. This indicates that TPE-PDI_4 exhibits a more favorable Lowest Unoccupied Molecular Orbital (LUMO) level than that of PCBM. Note that this high performance of non-fullerene OSCs is achieved without using any single or binary additives or special interlayers, which simplifies device processing and optimization. The external quantum efficiency (EQE) spectrum of PBDTT-F-TT:TPE-PDI_4 based cells is shown in Figure 3d. The maximum EQE value is achieved at 540 nm, which corresponds to the absorption peak of TPE-PDI_4. This indicates that the light absorption of the TPE-PDI_4 acceptor makes a significant contribution to the light absorption and thus current generation of the solar cell. A key feature of SM acceptors compared with fullerenes is their excellent light absorption properties, which can be used to complement the absorption of the donor polymers.

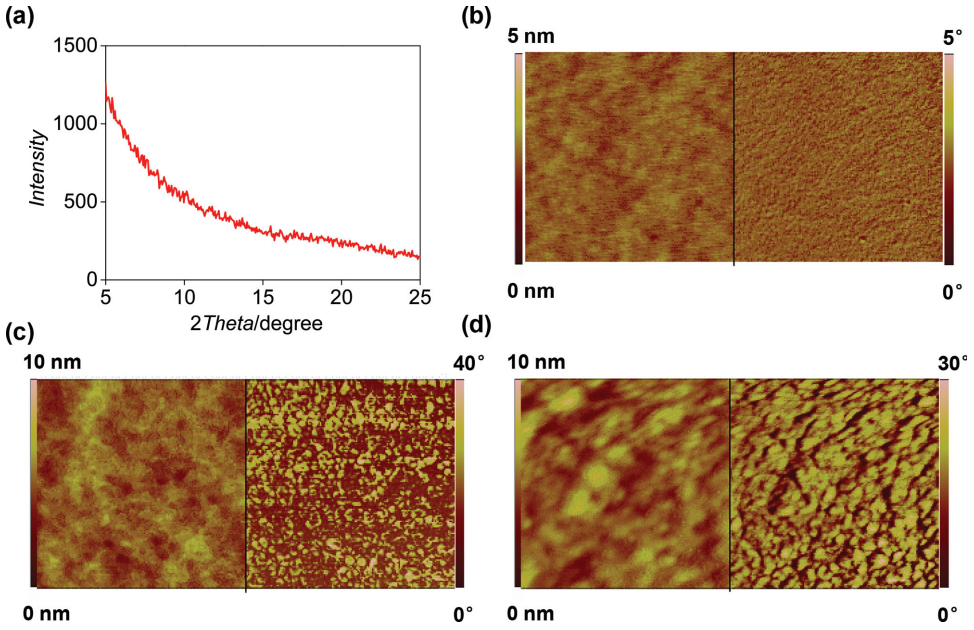

Figure 2. a) X-ray diffraction (XRD) pattern of a TPE-PDI$_4$ film; b–d) AFM images (1 × 1 μm) of b) a neat TPE-PDI$_4$ film, c) a PBDTT-F-TT:TPE-PDI$_4$ film, and d) a PBDTT-F-TT:BP-PDI$_2$ film. The height and phase images are displayed on the left and right sides, respectively.

The high performance of TPE-PDI$_4$-based cells can be attributed to their combination of amorphous film properties and reasonably good electron-transport ability, both of which are enabled by TPE-PDI$_4$'s 3D molecular structure. To further elucidate this aspect, TPE-PDI$_4$ is compared with a PDI dimer connected with a biphenyl-bridging group named BP-PDI$_2$ (Figure 3b). While the electron mobility of TPE-PDI$_4$ (determined by the SCLC method) is about 1×10^{-3} cm^2 V^{-1} s^{-1}, that of BP-PDI$_2$ is about 2×10^{-4} cm^2 V^{-1} s^{-1}. This indicates that the large 3D structure of TPE-PDI$_4$ enables a significantly higher electron mobility

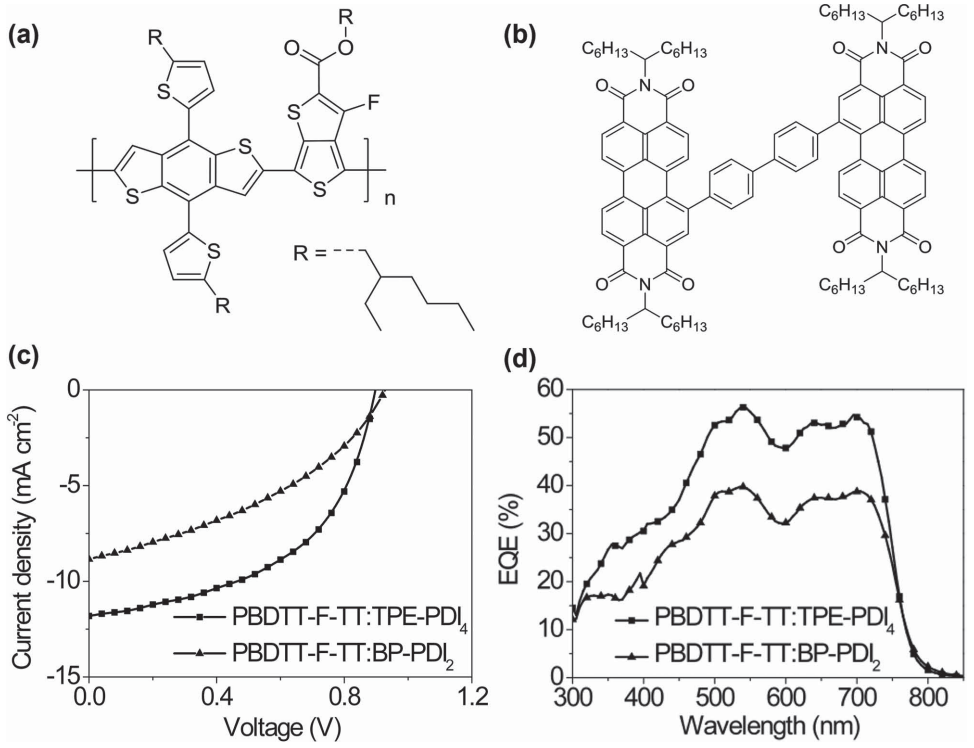

Figure 3. a) Chemical structure of the donor polymer PBDTT-F-TT; b) Chemical structure of BP-PDI$_2$; c) *J–V* curves of BHJ solar cells fabricated from PBDTT-F-TT:TPE-PDI$_4$ and PBDTT-F-TT:BP-PDI$_2$ under AM 1.5G irradiation at 100 mW cm^{-2}; and d) External quantum efficiency spectra of the devices.

Table 1. Performances of OSCs based on PBDTT-F-TT:TPE-PDI$_4$ or BP-PDI$_2$. The values in parentheses stand for the average PCEs from over 10 devices.

Acceptor	V_{OC} [V]	J_{SC} [mA cm^{-2}]	FF	PCE [%]
TPE-PDI$_4$	0.91	11.7	0.52	5.53 (5.44)
BP-PDI$_2$	0.93	8.6	0.39	3.13 (2.42)

Table 2. Energy levels and optical properties of TPE-PDI$_4$ and BP-PDI$_2$.

	λ_{max} [nm][a)]	λ_{onset} [nm][a)]	LUMO [eV][b)]	$E_{g,opt}$ [eV][c)]	HOMO [eV][d)]
TPE-PDI$_4$	537	604	−3.72	2.05	−5.77
BP-PDI$_2$	534	592	−3.72	2.09	−5.81

[a)]Obtained from film absorption data; [b)]Measured by cyclic voltammetry; [c)]Estimated based on film absorption onset; [d)]Calculated by using LUMO and $E_{g,opt}$.

than that of the dimer with a linear 2D structure. In addition, AFM images show that the blend film of PBDTT-F-TT:BP-PDI$_2$ has a significantly larger domain size (60–80 nm) (Figure 2d) than that of the PBDTT-F-TT:TPE-PDI$_4$ film (20 nm) (Figure 2c). The different domain sizes can be partially attributed to the different aggregation properties of BP-PDI$_2$ and TPE-PDI$_4$. (Note that the domain size in a BHJ film could be affected by many other factors related to the properties of the donor, acceptor, and solvents.) The higher electron mobility of TPE-PDI$_4$ can be attributed to its unique 3D molecular structure that is likely to facilitate the formation of a 3D charge-transporting network. The smaller domain size and amorphous nature of TPE-PDI$_4$ are partially due to the highly twisted molecular structure originating from the TPE core, which is the key reason for TPE-PDI$_4$ exhibiting very weak intermolecular interaction and molecular aggregation despite its large structure and molecular weight. As a result of the less favorable morphology and lower electron mobility of BP-PDI$_2$, the efficiencies of PBDTT-F-TT:BP-PDI$_2$-based cells are only about 3.1% (Table 1).

In terms of electrochemical and optical properties, the Highest Occupied Molecular Orbital (HOMO) and LUMO levels of TPE-PDI$_4$ are estimated to be −5.77 and −3.72 eV respectively, based on the results of cyclic voltammetry (CV) measurements and the optical bandgap of the film (**Table 2**). These values are similar to those of the BP-PDI$_2$ and other PDI dimers reported in the literature.[19] Further studies on TPE-PDI$_4$ have been carried out by comparing the UV–Vis absorption spectra of TPE-PDI$_4$ in solutions and as films. The absorption peak of TPE-PDI$_4$ in solution is at 530 nm, which is also comparable to that of BP-PDI$_2$ (**Figure 4**a). The absorption spectra of TPE-PDI$_4$ solutions at different temperatures are nearly identical (Figure 4b), which indicates that TPE-PDI$_4$ is not aggregated in solution. Reported PDI dimers with phenyl-ring-bridging groups all exhibit twisted structures, which result in minimal conjugation between the two PDI units.[19] The LUMO level of these dimers is thus comparable to that of the PDI monomer. The HOMO, LUMO, and UV–Vis spectrum of TPE-PDI$_4$ being similar to those of PDI dimers (e.g., BP-PDI$_2$ and phenyl-bridged PDI dimer[19]) indicates that there is negligible conjugation between the four PDI units in TPE-PDI$_4$ due to the highly twisted nature of the TPE core. In addition, the absorption spectrum of a neat TPE-PDI$_4$ film exhibits a very small redshift of about 10 nm, which is comparable to the solution-to-film redshift of BP-PDI$_2$. These results indicate that there is a minimal amount of conjugation between the PDI units for TPE-PDI$_4$ in the solid state, which would otherwise lower the LUMO level of the acceptor and thus the V_{OC} of the OSCs.[19] As a result, a high LUMO level of TPE-PDI$_4$ and an impressive V_{OC} of 0.91 V have been achieved, significantly higher than the corresponding PBDTT-F-TT:PCBM cells.[36] This is an important advantage of using SM acceptors, as it is easier to tune the LUMO level of SM materials to achieve a higher V_{OC} for the same donor polymer.

The ^{1}H NMR spectrum of TPE-PDI$_4$ in $CDCl_3$ solution shows sharp peaks in the aromatic region. For instance, the protons on the phenyl rings clearly show as two pairs of sharp doublets at 7.56 and 7.51 ppm (Figure S1, Supporting Information) representing four protons on each TPE phenyl ring. The other peaks in the aromatic region correspond to the seven protons on a PDI unit. This indicates that all phenyl and PDI units are freely rotating in solution and the protons on one phenyl-PDI wing have identical chemical environments to the corresponding protons on the other three wings. These data together indicate that the phenyl and PDI units of TPE-PDI$_4$ can freely rotate and that TPE-PDI$_4$ is disaggregated in solution.

Regarding conformational isomers, it is well known that TPE can form two isomers in the solid state with the phenyl rings tilting in two different directions.[37] When the phenyl

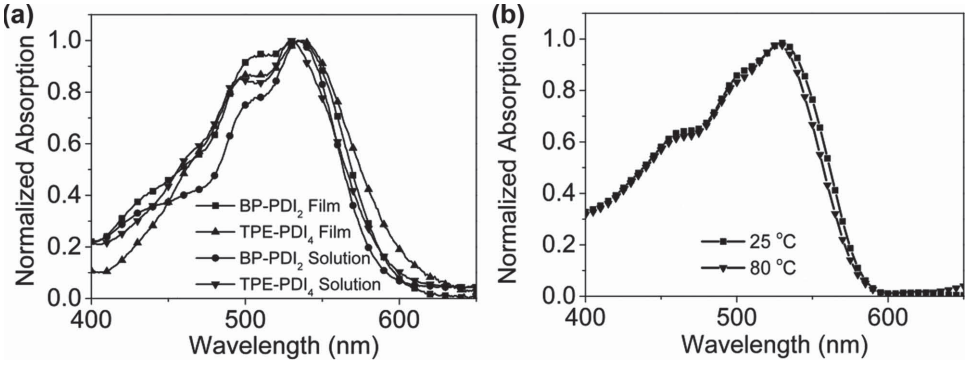

Figure 4. UV–vis absorption spectra of a) TPE-PDI$_4$ and BP-PDI$_2$ as films and in solutions; b) TPE-PDI$_4$ in a solution at 25 and 80 °C.

rings on TPE are replaced by or substituted with asymmetric-aromatic groups, the resulting molecular structure has many more forms of conformational isomers in the solid state.[33] The four wings in TPE-type molecules can freely rotate in solutions, but the rotation is restricted in the solid state. When TPE-type molecules transition from the solution state to the solid state, each of the four wings on the TPE core can tilt in one of the two possible directions. If the "wing" has an asymmetric structure, the four wings tilting in two possible directions independently will result in a large number of conformational isomers, as shown previously.[33] Similarly, TPE-PDI_4 can also form several possible isomers, with three possible conformations as shown in Figure 1c-e. In DFT calculations, three different conformational isomers of TPE-PDI_4 (with the PDI wings tilting in different directions) were used as the initial input for optimal geometry calculations. Three different initial inputs led to three different locally optimal conformations of TPE-PDI_4, with the PDI wings tilting in different directions. The energy difference between these locally optimal conformations was very small (< 4.78 kJ mol^{-1}), indicating that TPE-PDI_4 may exhibit multiple structural conformations in the solid state. Considering that the TPE core has two additional possible isomeric conformations independent of the tilting directions of the PDI wings,[37] there should be more than three conformational isomers for TPE-PDI_4.

To conclude, the unique 3D molecular structure of TPE-PDI_4 enables several interesting and beneficial properties. First, due to the highly twisted nature of the TPE core, TPE-PDI_4 exhibits weak molecular aggregation, forms smooth and amorphous neat films, and contributes to the formation of a BHJ morphology featuring a small domain size. The 3D structure of TPE-PDI_4 facilitates the formation of a 3D charge-transport network and thus enables a reasonably good electron-transport ability. These advantageous features of TPE-PDI_4 are clearly demonstrated by comparing TPE-PDI_4 with BP-PDI_2, which has a 2D molecular structure. While TPE-PDI_4 can form BHJ films with smaller feature sizes than those formed by BP-PDI_2, TPE-PDI_4 also exhibits a significantly greater electron-transport ability. Lastly, CV and UV–Vis data support that there is negligible conjugation between the four PDI units in TPE-PDI_4, which allows TPE-PDI_4 to maintain a relatively high LUMO level and achieve OSCs with a higher V_{OC} than that of the corresponding PCBM-based cells. All these positive factors combined led to high-performance non-fullerene OSCs with a 5.53% power-conversion efficiency. Our work offers a new molecular design approach to develop SM materials with 3D structures, based on which high-efficiency non-fullerene OSCs could be obtained.

Supporting Information

Supporting Information is available from the Wiley Online Library or from the author.

Acknowledgements

Y.L., C.M., and K.J. contributed equally to this work. The work was partially supported by the National Basic Research Program of China (973 Program; 2013CB834701), the Hong Kong Innovation and Technology Commission (ITS/354/12), the Hong Kong Research Grants Council (T23–407/13-N, N_HKUST623/13, and 606012) and the National Science Foundation of China (#21374090).

Received: September 9, 2014
Revised: October 15, 2014
Published online: November 27, 2014

[1] G. Yu, J. Gao, J. C. Hummelen, F. Wudl, A. J. Heeger, *Science* **1995**, *270*, 1789.
[2] H. Y. Chen, J. H. Hou, S. Q. Zhang, Y. Y. Liang, G. W. Yang, Y. Yang, L. P. Yu, Y. Wu, G. Li, *Nat. Photon.* **2009**, *3*, 649.
[3] X. G. Guo, N. J. Zhou, S. J. Lou, J. Smith, D. B. Tice, J. W. Hennek, R. P. Ortiz, J. T. L. Navarrete, S. Y. Li, J. Strzalka, L. X. Chen, R. P. H. Chang, A. Facchetti, T. J. Marks, *Nat. Photon.* **2013**, *7*, 825.
[4] Z. C. He, C. M. Zhong, S. J. Su, M. Xu, H. B. Wu, Y. Cao, *Nat. Photon.* **2012**, *6*, 591.
[5] J. B. You, L. T. Dou, K. Yoshimura, T. Kato, K. Ohya, T. Moriarty, K. Emery, C. C. Chen, J. Gao, G. Li, Y. Yang, *Nat. Commun.* **2013**, *4*, 1446.
[6] J. T. Bloking, T. Giovenzana, A. T. Higgs, A. J. Ponec, E. T. Hoke, K. Vandewal, S. Ko, Z. Bao, A. Sellinger, M. D. McGehee, *Adv. Energy Mater.* **2014**, *4*, 1301426.
[7] Y. Lin, Y. Li, X. Zhan, *Chem. Soc. Rev.* **2012**, *41*, 4245.
[8] V. D. Mihailetchi, J. K. J. van Duren, P. W. M. Blom, J. C. Hummelen, R. A. J. Janssen, J. M. Kroon, M. T. Rispens, W. J. H. Verhees, M. M. Wienk, *Adv. Funct. Mater.* **2003**, *13*, 43.
[9] S. Cho, J. H. Seo, K. Lee, A. J. Heeger, *Adv. Funct. Mater.* **2009**, *19*, 1459.
[10] L. T. Dou, J. B. You, Z. R. Hong, Z. Xu, G. Li, R. A. Street, Y. Yang, *Adv. Mater.* **2013**, *25*, 6642.
[11] Y. He, Y. Li, *Phys. Chem. Chem. Phys.* **2011**, *13*, 1970.
[12] A. F. Eftaiha, J. P. Sun, I. G. Hill, G. C. Welch, *J. Mater. Chem. A* **2014**, *2*, 1201.
[13] F. G. Brunetti, X. Gong, M. Tong, A. J. Heeger, F. Wudl, *Angew. Chem Int. Ed.* **2010**, *49*, 532.
[14] J. T. Bloking, X. Han, A. T. Higgs, J. P. Kastrop, L. Pandey, J. E. Norton, C. Risko, C. E. Chen, J.-L. Brédas, M. D. McGehee, A. Sellinger, *Chem. Mater.* **2011**, *23*, 5484.
[15] S. Rajaram, R. Shivanna, S. K. Kandappa, K. S. Narayan, *J. Phys. Chem. Lett.* **2012**, *3*, 2405.
[16] A. Sharenko, C. M. Proctor, T. S. van der Poll, Z. B. Henson, T.-Q. Nguyen, G. C. Bazan, *Adv. Mater.* **2013**, *25*, 4403.
[17] Y. Zhou, L. Ding, K. Shi, Y. Z. Dai, N. Ai, J. Wang, J. Pei, *Adv. Mater.* **2012**, *24*, 957.
[18] Y. Zhou, Y. Z. Dai, Y. Q. Zheng, X. Y. Wang, J. Y. Wang, J. Pei, *Chem. Commun.* **2013**, *49*, 5802.
[19] Q. F. Yan, Y. Zhou, Y. Q. Zheng, J. Pei, D. H. Zhao, *Chem. Sci.* **2013**, *4*, 4389.
[20] X. Zhang, Z. Lu, L. Ye, C. Zhan, J. Hou, S. Zhang, B. Jiang, Y. Zhao, J. Huang, S. Zhang, Y. Liu, Q. Shi, Y. Liu, J. Yao, *Adv. Mater.* **2013**, *25*, 5791.
[21] Y. Lin, Y. Wang, J. Wang, J. Hou, Y. Li, D. Zhu, X. Zhan, *Adv. Mater.* **2014**, *26*, 5137.
[22] W. Jiang, L. Ye, X. G. Li, C. Y. Xiao, F. Tan, W. C. Zhao, J. H. Hou, Z. H. Wang, *Chem. Commun.* **2014**, *50*, 1024.
[23] Z. H. Lu, B. Jiang, X. Zhang, A. L. Tang, L. L. Chen, C. L. Zhan, J. N. Yao, *Chem. Mater.* **2014**, *26*, 2907.
[24] Y. Zang, C. Z. Li, C. C. Chueh, S. T. Williams, W. Jiang, Z. H. Wang, J. S. Yu, A. K. Jen, *Adv. Mater.* **2014**, *26*, 5708.
[25] Z. Mao, W. Senevirathna, J.-Y. Liao, J. Gu, S. V. Kesava, C. Guo, E. D. Gomez, G. Sauvé, *Adv. Mater.* **2014**, *26*, 6290.

[26] X. Zhan, Z. a. Tan, B. Domercq, Z. An, X. Zhang, S. Barlow, Y. Li, D. Zhu, B. Kippelen, S. R. Marder, *J. Am. Chem. Soc.* **2007**, *129*, 7246.
[27] T. Earmme, Y.-J. Hwang, N. M. Murari, S. Subramaniyan, S. A. Jenekhe, *J. Am. Chem. Soc.* **2013**, *135*, 14960.
[28] Y. Zhou, T. Kurosawa, W. Ma, Y. Guo, L. Fang, K. Vandewal, Y. Diao, C. Wang, Q. Yan, J. Reinspach, J. Mei, A. L. Appleton, G. I. Koleilat, Y. Gao, S. C. B. Mannsfeld, A. Salleo, H. Ade, D. Zhao, Z. Bao, *Adv. Mater.* **2014**, *26*, 3767.
[29] C. Mu, P. Liu, W. Ma, K. Jiang, J. Zhao, K. Zhang, Z. Chen, Z. Wei, Y. Yi, J. Wang, S. Yang, F. Huang, A. Facchetti, H. Ade, H. Yan, *Adv. Mater.* **2014**, *26*, 7224.
[30] D. Mori, H. Benten, I. Okada, H. Ohkita, S. Ito, *Energy Environ. Sci.* **2014**, *7*, 2939.
[31] H. Tong, Y. N. Hong, Y. Q. Dong, M. Haussler, J. W. Y. Lam, Z. Li, Z. F. Guo, Z. H. Guo, B. Z. Tang, *Chem. Commun.* **2006**, 3705.
[32] Y. N. Hong, J. W. Y. Lam, B. Z. Tang, *Chem. Commun.* **2009**, 4332.
[33] S. Pogodin, N. Assadi, I. Agranat, *Struct. Chem.* **2013**, *24*, 1747.
[34] C. Huang, S. Barlow, S. R. Marder, *J. Org. Chem.* **2011**, *76*, 2386.
[35] C. Li, H. Wonneberger, *Adv. Mater.* **2012**, *24*, 613.
[36] S. H. Liao, H. J. Jhuo, Y. S. Cheng, S. A. Chen, *Adv. Mater.* **2013**, *25*, 4766.
[37] K. Tanaka, D. Fujimoto, T. Oeser, H. Irngartinger, F. Toda, *Chem. Commun.* **2000**, 413.